

The Aryl Hydrocarbon Receptor-interacting Protein (AIP) Is Required for Dioxin-induced Hepatotoxicity but Not for the Induction of the *Cyp1a1* and *Cyp1a2* Genes^{*[5]}

Received for publication, April 8, 2010, and in revised form, September 7, 2010. Published, JBC Papers in Press, September 9, 2010, DOI 10.1074/jbc.M110.132043

Manabu Nukaya^{‡§1}, Bernice C. Lin^{‡1}, Edward Glover[‡], Susan M. Moran[‡], Gregory D. Kennedy[§], and Christopher A. Bradfield^{‡2}

From the [‡]McArdle Laboratory for Cancer Research, University of Wisconsin, School of Medicine and Public Health, Madison, Wisconsin 53706 and the [§]Department of Surgery, University of Wisconsin, School of Medicine and Public Health, Madison, Wisconsin 53706

The aryl hydrocarbon receptor (AHR) plays an essential role in the toxic response to environmental pollutants such as 2,3,7,8-tetrachlorodibenzo-*p*-dioxin (dioxin), in the adaptive up-regulation of xenobiotic metabolizing enzymes, and in hepatic vascular development. In our model of AHR signaling, the receptor is found in a cytosolic complex with a number of molecular chaperones, including Hsp90, p23, and the aryl hydrocarbon receptor-interacting protein (AIP), also known as ARA9 and XAP2. To understand the role of AIP in adaptive and toxic aspects of AHR signaling, we generated a conditional mouse model where the *Aip* locus can be deleted in hepatocytes. Using this model, we demonstrate two important roles for the AIP protein in AHR biology. (i) The expression of AIP in hepatocytes is essential to maintain high levels of functional cytosolic AHR protein in the mammalian liver. (ii) Expression of the AIP protein is essential for dioxin-induced hepatotoxicity. Interestingly, classical AHR-driven genes show differential dependence on AIP expression. The *Cyp1b1* and *Ahrr* genes require AIP expression for normal up-regulation by dioxin, whereas *Cyp1a1* and *Cyp1a2* do not. This differential dependence on AIP provides evidence that the mammalian genome contains more than one class of AHR-responsive genes and suggests that a search for AIP-dependent, AHR-responsive genes may guide us to the targets of the dioxin-induced hepatotoxicity.

The aryl hydrocarbon receptor (AHR)³ mediates the toxic effects of persistent environmental pollutants/ligands such as chlorinated-dibenzo-*p*-dioxins (e.g. 2,3,7,8-tetrachlorodibenzo-*p*-dioxin or "dioxin") (1–3). In the classic signaling model, ligand binds to the AHR in the cytosol, and the activated

receptor translocates into the nucleus, where the AHR can dimerize with its transcriptional partner, the AHR nuclear translocator (ARNT) (1, 2). Within the nucleus, the AHR/ARNT heterodimer binds to cognate enhancers known as dioxin-responsive elements (DREs) (1, 2, 4, 5). This binding leads to the transcriptional up-regulation of genes encoding xenobiotic metabolizing enzymes such as *Cyp1a1*, *Cyp1a2*, and *Cyp1b1*, as well as a negative regulator of signaling known as the AHR repressor (*Ahrr*) (1, 2, 4, 6, 7). This pathway is thought to represent an adaptive metabolic response that allows for the detoxification of a wide variety of environmental contaminants with polycyclic aromatic structures (1, 2, 4–6). The AHR also mediates the toxic effects of dioxins, including endpoints such as tumor promotion, chloracne, thymic involution, teratogenesis, and hepatocellular damage (3). Recent experiments have demonstrated that the AHR also plays an essential role in normal vascular development as both *Ahr* and *Arnt* mutant mice display a failure in the postnatal closure of a hepatovascular porto-caval shunt known as the ductus venosus (DV) (8–12). This fetal hepatic vascular structure normally shunts blood flow from the umbilical vein to the inferior vena cava bypassing the liver during development (8–12).

The cytosolic AHR has been shown to exist in a complex with the 90-kDa heat shock protein (Hsp90), p23, and the aryl hydrocarbon receptor-interacting protein (AIP, also known as ARA9 (AHR-associated protein 9) and XAP2 (hepatitis B virus X-activating protein 2)) (13–15). The AIP protein, which is structurally related to the FK506-binding protein class of immunophilins, was originally identified as a protein that interacts with the AHR and the hepatitis B virus protein X in yeast two-hybrid screens (13, 16, 17). Additional studies revealed that the AIP acts as a chaperone, presumably maintaining properly folded AHR in the cytosol and improving the stability, subcellular localization, and ligand binding ability of the receptor *in vivo* (18–21).

To understand the role of AIP in normal development, we previously generated an *Aip* null allele (designated *Aip*^{-/-}) (22). Interestingly, the *Aip*^{-/-} mice display severe cardiovascular defects, including heart deformation; double outlet right ventricle; ventricular-septal defects; and pericardial edema (22). Because *Ahr* null mice display normal heart development, we concluded that AIP plays an essential role in cardiovascular development in a manner that is independent of its role in AHR

* This work was supported, in whole or in part, by National Institutes of Health Grants R01-ES-06883, R37-ES-05703, T32-CA-009135, P30-CA-014520 (to C. A. B.), and K08-ES-017283 (to G. D. K.).

[5] The on-line version of this article (available at <http://www.jbc.org>) contains a supplemental figure.

¹ Both authors contributed equally to this work.

² To whom correspondence should be addressed: University of Wisconsin School of Medicine and Public Health, McArdle Laboratory for Cancer Research, 1400 University Ave., Madison, WI 53706. Tel.: 608-262-2024; Fax: 608-262-2824; E-mail: bradfield@oncology.wisc.edu.

³ The abbreviations and trivial names used are: AHR, aryl hydrocarbon receptor; ARNT, AHR nuclear translocator; AIP, AHR-interaction protein; ALT, alanine aminotransferase; CYP, cytochrome P450; dioxin, 2,3,7,8-tetrachlorodibenzo-*p*-dioxin; DRE, dioxin-responsive element; DV, ductus venosus.

Adaptive and Toxic Role of AIP in Hepatocytes

signaling (8, 23). To overcome the embryonic lethality due to global *Aip* loss, we generated a hypomorphic *Aip* mouse model (designated *Aip*^{fxneo/fxneo}), which expressed ~10% AIP protein as compared with wild-type mice (24). The *Aip*^{fxneo/fxneo} mice did not show heart defects nor significant embryonic lethality, yet they did display a high incidence of patent DV, similar to *Ahr* mutant mice and the *Arnt* mutant mice (8–12, 24). This finding led us to conclude that AIP is essential for the developmental role of AHR. Because these AIP hypomorphs displayed aberrant first pass clearance of xenobiotics resulting from the patent DV, this model was not applicable to studies of AHR-mediated dioxin toxicity or adaptive metabolic pathways.

To understand the adaptive and toxicological roles of AIP, we developed a conditional null allele of *Aip* that would circumvent cardiovascular and hepatic vascular roles. Previously, we demonstrated that when a conditional null allele of *Ahr* was deleted in hepatocytes, the developmental issues related to patent DV were avoided (25). Using this hepatocyte AHR null model with normal vasculature, we were able to examine the role of the hepatocyte AHR in the up-regulation of xenobiotic metabolism and in dioxin-induced toxicity in the liver (25). Given the prior success of this strategy, we generated mice harboring an *Aip* null allele in hepatocytes to investigate the role of the AIP protein in the developmental, toxic, and adaptive pathways of AHR biology.

MATERIALS AND METHODS

Generation of Conditional *Aip*^{fx/fx} Mice—To generate the conditional *Aip*^{fx/fx} allele (fx; flanked by *lox-p* sites or “floxed”), we used mice harboring the constitutive hypomorphic *Aip* allele that was generated previously (designated *Aip*^{fxneo}) (see Fig. 1A) (24). To excise the neomycin resistance cassette (*Neo*), the *Aip*^{fxneo/+} mice were crossed to *Flp*^{ROSA26S} mice (a *Flp* recombinase-expressing strain; Gt(ROSA)26Sor^{tm1(FLP1)Dym}, The Jackson Laboratory, Bar Harbor, ME) (26, 27). The excision of the *Neo* cassette was confirmed by PCR genotyping. The PCR was performed by using a forward primer (OL4208, 5'-CAC-CACCTGTCAATCCCCACTG-3'), a reverse primer (OL4635, 5'-CTCCCACTGACTACCAAGC-3') and a reverse primer for *Neo* (OL6032, 5'-CTGCTCTTTACTGAAGGCTC-3'). The 135-, 460-, and 220-bp PCR products corresponded to WT (*Aip*⁺), *Aip*^{fxneo}, and *Aip*^{fx} alleles, respectively.

Generation of Hepatocyte-specific *Aip* Null Mice—To obtain mice harboring the *Aip* null allele in hepatocytes, the conditional *Aip*^{fx/fx} mice were crossed to *Cre*^{alb} mice expressing a *Cre* (P1 bacteriophage cyclization recombination recombinase) transgene driven by the albumin promoter (*Cre*^{alb}, strain name: B6.Cg-Tg(Albcre)21Mgn_J, The Jackson Laboratory) (28). The resultant heterozygous *Aip*^{fx/+} mice carrying the *Cre*^{alb} transgene (*Aip*^{fx/+}*Cre*^{alb}) were backcrossed to homozygous *Aip*^{fx} mice (*Aip*^{fx/fx}) to generate the *Aip*^{fx/fx} mice with *Cre*^{alb} transgene (*Aip*^{fx/fx}*Cre*^{alb}) and their littermate controls without the *Cre*^{alb} transgene (*Aip*^{fx/fx}). To confirm hepatocyte-specific excision of the target locus, we employed PCR genotyping by using the forward primer for *Aip*^{fx} allele (OL4208), the forward primer for *Aip* null allele (OL4672, 5'-GGTGGCCAGAAATCATGAC-3'), and the reverse primer (OL4635). These primers amplified a 220-bp band from *Aip*^{fx} allele and a 200-bp band from *Aip* null allele.

Animals—Mice were housed in a selective pathogen-free facility on corn cob bedding with food and water *ad libitum* following the protocol established by the University of Wisconsin Medical School Animal Care and Use Committee. The *Cre*^{alb} and *Flp*^{ROSA26} mice were backcrossed to C57BL/6J mice for >10 generations prior to their use in these experiments. The *Aip*^{fxneo} mice were backcrossed three times to the C57BL/6J strain prior to their use. The *Aip*^{fx} alleles were backcrossed to C57BL/6J mice for four generations prior to use. All strains of mice were selected for homozygosity for the *Ahr*^{b1} allele (29).

Assessment of DV Patency—Male mice (8 weeks old) were used for monitoring DV closure. Closure was assessed by perfusion of the liver with 0.4% trypan blue dye as described previously (10–12). The *Ahr* null mice (*Ahr*^{-/-}) were employed as positive controls for DV patency (8).

Treatment and Toxicology Studies—Male mice (8-week old) were injected with a single intraperitoneal dose of 2,3,7,8-tetrachlorodibenzo-*p*-dioxin (dioxin) (64 μg/kg of total body weight) dissolved in corn oil or corn oil alone as vehicle control (30). 5 days after the injection, mice were sacrificed by CO₂ euthanasia. The serum alanine aminotransferase (ALT) assay was carried out as described previously (30). The liver, kidney, lung, heart, spleen, and thymus were removed and weighed. These tissues were used for preparation of genomic DNA, total RNA, and cytosolic and microsomal proteins (10, 12, 30). The left liver lobe was sliced and fixed in 10% formalin in PBS. The paraffin-embedded sections were stained with hematoxylin and eosin. No patent DV was observed in the *Aip*^{fx/fx}*Cre*^{alb} mice used in toxicology experiments.

Gene Expression Analysis—Total liver RNA was prepared using the RNeasy Protect system (Qiagen, Valencia, CA). For the quantitative RT-PCR, total RNA was reverse-transcribed using the High Capacity cDNA reverse transcription kit (Applied Biosystems, Foster City, CA). Expression levels of AHR gene batteries were measured with TaqMan universal PCR master mix (Applied Biosystems) and custom-designed probes (assay ID: *Cyp1a1*, Mm00487218_m1; *Cyp1a2*, Mm00487224_m1; *Cyp1b1*, Mm00487229_m1; *Ahr*, Mm00477445_m1; β-actin, Mm01205647_g1). The expression levels were normalized to β-actin levels.

Protein Studies—The cytosolic and microsomal proteins were prepared from liver samples as described previously (25, 30). For the Western blot analysis, 150 μg of cytosolic protein or 50 μg of microsomal protein were loaded onto SDS-PAGE gels and transferred to Immobilon-P membranes by electrophoresis (Millipore, Bedford, MA). The AIP protein band was detected with a mouse monoclonal FK506-binding protein (FKBP) domain specific antibody (24). The AHR, ARNT, CYP1A1, and CYP1A2 proteins were detected as described previously (10, 12, 30). The β-actin protein was used as a loading control (Sigma-Aldrich). The CYP1B1 antibody was generous gift from Dr. C. R. Jefcoate (31).

In an effort to provide quantitation of the AHR and AIP protein levels based upon Western blotting, we measured Western blot signal intensity through densitometric scanning of the immunostained Immobilon-P membrane (LabWorks Image Acquisition and Analysis Software, Upland, CA). The AHR and

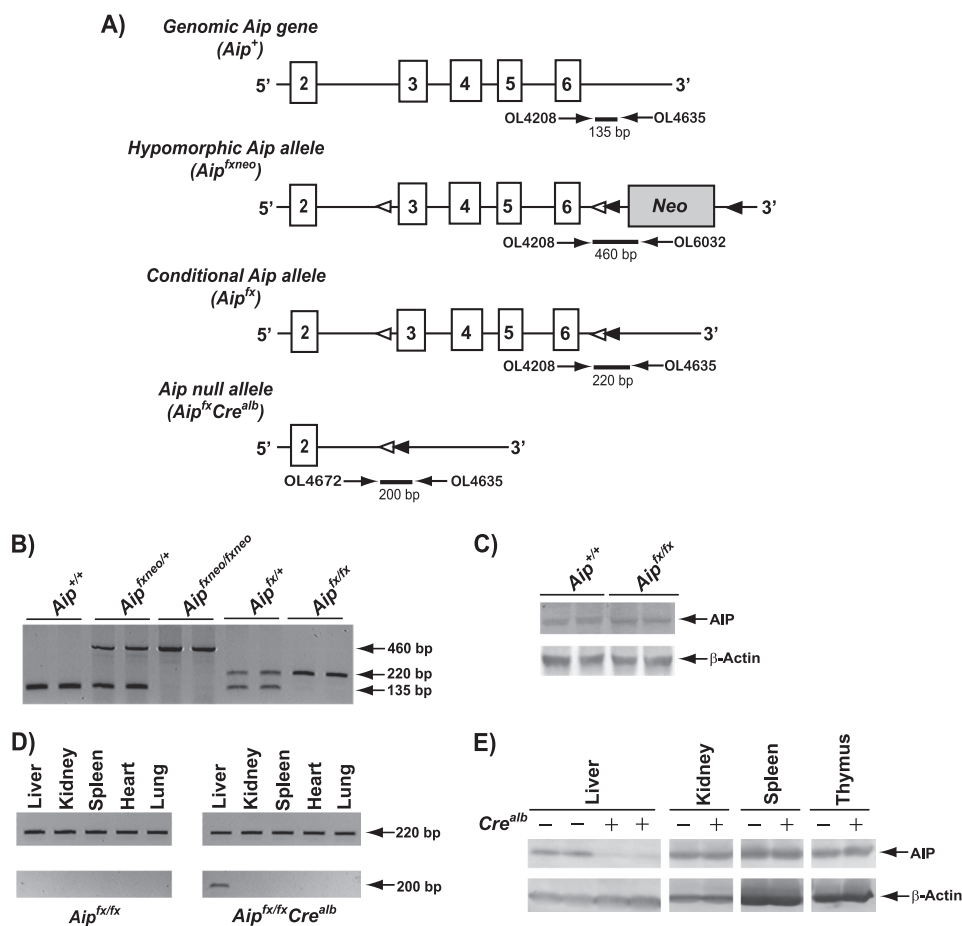


FIGURE 1. Generation of hepatocyte *Aip* null mice. *A*, genome maps of native mouse *Aip* gene (*Aip*⁺), hypomorphic *Aip* allele (*Aip*^{fxneo}), conditional *Aip* allele (*Aip*^{fx}), and hepatocyte *Aip* null allele (*Aip*^{fxCre^{alb}}). Open boxes, exon 2 to exon 6 of mouse *Aip* gene; Neo, neomycin resistance cassette; white arrowheads, *Lox-P* sites; black arrowheads, *Frt* sites; OL, PCR primers. *B*, PCR genotyping for *Aip*⁺, *Aip*^{fxneo}, and *Aip*^{fx} alleles. The 135-, 460-, and 220-bp PCR bands were amplified from *Aip*⁺, *Aip*^{fxneo}, and *Aip*^{fx} alleles, respectively. *C*, comparison of hepatic AIP protein levels between *Aip*^{+/+} and *Aip*^{fx/fx} mice. Cytosolic proteins were isolated from the livers of *Aip*^{+/+} and *Aip*^{fx/fx} mice. 150 μ g of cytosolic extracts were analyzed by Western blot using AIP-specific and β -actin antibody. *D*, PCR genotyping for *Aip*^{fx} and *Aip*^{fxCre^{alb}} alleles. The 220- and 200-bp bands were amplified from *Aip*^{fx} and *Aip*^{fxCre^{alb}} alleles. *E*, decrease of AIP protein levels in the livers of *Aip*^{fx/fxCre^{alb}} mice. Cytosolic proteins were isolated from liver, kidney, spleen, and thymus of *Aip*^{fx/fx} (*Cre^{alb}* (-)) and *Aip*^{fx/fxCre^{alb}} (*Cre^{alb}* (+)) mice. 150 μ g of cytosolic extracts were analyzed by Western blot using AIP-specific and β -actin antibody.

TABLE 1

Rate of DV patency in *Aip*^{fx/fx} and *Aip*^{fx/fxCre^{alb}} mice

Genotype	Patent DV	<i>n</i> ^a
	%	
<i>Aip</i> ^{fx/fx}	0	0/8
<i>Aip</i> ^{fx/fxCre^{alb}}	12.5	1/8
<i>Ahr</i> ^{-/-}	100	4/4

^a *n* = number of animals with DV/total animals.

AIP protein levels were then normalized to β -actin protein levels from the same lane on the gel.

Statistical Analysis—All statistical data are presented as mean \pm S.E. Intergroup comparisons were performed by one-way analysis of variance (30). Differences among groups were considered to be statistically significant when the *p* value was <0.05. Statistical analysis of genotype distribution was compared by χ^2 analysis (24).

RESULTS

Generation of Conditional *Aip*^{fx/fx} Mice—To obtain mice harboring the conditional *Aip*^{fx} allele, hypomorphic *Aip* mice

(*Aip*^{fxneo/fxneo}) were crossed to mice expressing *Flp* recombinase under control of the *ROSA26S* promoter, causing excision of the neomycin resistance cassette (*Neo*) (Fig. 1A) (26, 27). Following heritable loss of *Neo*, the resultant mice were backcrossed to C57BL/6J mice to remove the *Flp*^{ROSA26S} transgene. Excision of *Neo* was confirmed by PCR genotyping (Fig. 1B). The resulting progeny were interbred to obtain homozygous conditional *Aip*^{fx/fx} mice. The *Aip*^{fx/fx} mice displayed normal liver and heart development, which were indistinguishable from C57BL/6J mice (data not shown). In liver of the *Aip*^{fx/fx} mice, the AIP protein levels were not significantly different as compared with WT (*Aip*^{+/+}) mice (Fig. 1C).

Generation of Hepatocyte *Aip* Null Mice—To generate mice carrying the *Aip* null allele in hepatocytes, the *Aip*^{fx/fx} mice were crossed to mice expressing *Cre* recombinase under control of the albumin promoter (Fig. 1A) (28). The hepatocyte-specific deletion of *Aip* exons was confirmed by PCR genotyping (Fig. 1D). The resultant mice heterozygous for the *Aip*^{fx} allele and heterozygous for the *Cre^{alb}* transgene (*Aip*^{fx/+Cre^{alb}}) were backcrossed to the *Aip*^{fx/fx} mice, and homozygous *Aip*^{fx/fxCre^{alb}} mice carrying *Cre^{alb}* (*Aip*^{fx/fxCre^{alb}}) were generated. The *Aip*^{fx/fxCre^{alb}} mice were bred with the *Aip*^{fx/fx} mice, and the

offspring were employed in experiments. Analysis of the genotypes of progeny indicated that the birth ratio of *Aip*^{fx/fx} and *Aip*^{fx/fxCre^{alb}} mice was consistent with simple Mendelian segregation of a viable allele (*i.e.* *Aip*^{fx/fx}, 46% (27/59); *Aip*^{fx/fxCre^{alb}}, 54% (32/59) ($\chi^2 = 0.628$)). Semiquantitative analysis of Western blotting using densitometric scanning of band signal intensity indicated that levels of AIP protein in livers of *Aip*^{fx/fxCre^{alb}} mice were reduced greater than 85% as compared with the *Aip*^{fx/fx} mice (Fig. 1E). Consistent with the specificity of the *Cre^{alb}* promoter, AIP protein levels in kidney, spleen, and thymus were not significantly different between the two groups (Fig. 1E).

Phenotype of *Aip*^{fx/fxCre^{alb}} Mice—Previously we demonstrated that 5/6 mice homozygous for the hypomorphic *Aip* allele (*Aip*^{fxneo/fxneo}) displayed a patent DV (24). To examine whether excision of *Neo* circumvents the high frequency of DV patency, we perfused the portal vein with trypan blue dye and observed the status of DV in *Aip*^{fx/fx} mice. No *Aip*^{fx/fx} mice displayed a patent DV (number of animals with DV/total animals = 0/8) (Table 1). To investigate a role of hepato-

Adaptive and Toxic Role of AIP in Hepatocytes

TABLE 2

Impact of deletion of hepatocyte AIP on dioxin-induced toxicity

Mice were treated with corn oil or 64 $\mu\text{g}/\text{kg}$ of dioxin and sacrificed five days after the single i.p. injection. Each group contains six mice. All statistical data are presented as mean \pm S.E.

Genotype	Treatment	Body weight	Liver weight		Thymus weight		Serum ALT activity (units/liter)
			Wet	Relative (% of body weight)	Wet	Relative (% of body weight)	
<i>Aip^{fx/fx}</i>	Corn oil	24.13 \pm 0.80	1.04 \pm 0.16	4.31 \pm 0.59	41.56 \pm 2.50	0.17 \pm 0.01	38.3 \pm 8.1
	Dioxin	24.20 \pm 1.68	1.48 \pm 0.12 ^a	6.15 \pm 0.42 ^a	17.25 \pm 3.09 ^a	0.07 \pm 0.01 ^a	277.1 \pm 179.2 ^a
<i>Aip^{fx/fx}Cre^{alb}</i>	Corn oil	21.68 \pm 1.99 ^a	0.87 \pm 0.03 ^a	4.01 \pm 0.30	34.77 \pm 6.64	0.16 \pm 0.02	32.5 \pm 11.3
	Dioxin	22.30 \pm 1.88	1.28 \pm 0.07 ^a	5.79 \pm 0.66 ^a	18.40 \pm 1.46 ^a	0.08 \pm 0.01 ^a	55.0 \pm 25.5

^a Significantly different relative to the corn oil-treated *Aip^{fx/fx}* mice ($p < 0.05$).

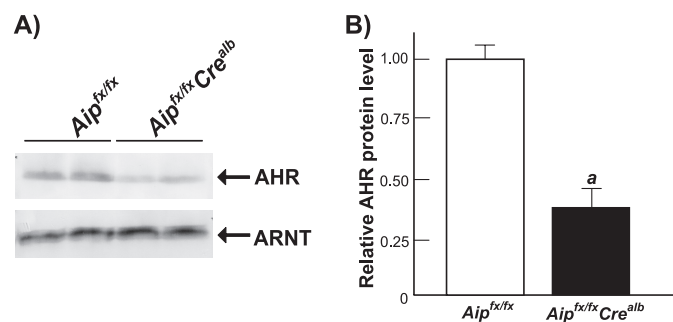


FIGURE 2. Decreased AHR protein levels in the livers of *Aip^{fx/fx}Cre^{alb}* mice. Cytosolic proteins were isolated from the liver of *Aip^{fx/fx}* and *Aip^{fx/fx}Cre^{alb}* mice. **A**, 150 μg of cytosolic extracts were analyzed by Western blot using mouse AHR- and ARNT-specific antibody. **B**, relative AHR protein levels in the livers of *Aip^{fx/fx}* and *Aip^{fx/fx}Cre^{alb}* mice. The AHR and β -actin protein levels were determined by semiquantitative analysis of Western blot intensity. The AHR protein levels were normalized to β -actin protein levels. The result was expressed as relative AHR protein level as compared with *Aip^{fx/fx}* mice. Each group contained four mice. Error bars represent S.E. *a*, significantly different relative to the *Aip^{fx/fx}* mice ($p < 0.05$).

cyte AIP in the DV closure, the perfusion assay was performed in male *Aip^{fx/fx}Cre^{alb}* mice. The *Aip^{fx/fx}Cre^{alb}* mice displayed 12.5% incidence of patent DV in adulthood ($n = 1/8$) (Table 1).

Other outward phenotypes, including male/female ratio and fertility, were not significantly different between *Aip^{fx/fx}* and *Aip^{fx/fx}Cre^{alb}* mice (data not shown). Interestingly, we have observed that the *Aip^{fx/fx}Cre^{alb}* mice are $\sim 10\%$ smaller than their littermate controls (*Aip^{fx/fx}*) at 8 weeks (Table 2). Despite this modest reduction in body weight, the relative organ weights remain proportional, and no marked differences in histology of the liver have been noted (Table 2 and supplemental material).

Decreased AHR Protein Levels in Livers of *Aip^{fx/fx}Cre^{alb}* Mice—To examine the influence of *Aip* deletion on components of AHR signaling, we examined the expression of the AHR and ARNT protein levels by Western blot from livers of *Aip^{fx/fx}* and *Aip^{fx/fx}Cre^{alb}* mice (Fig. 2A). Although ARNT protein levels were not significantly different between the two groups, the amount of AHR protein was markedly reduced (Fig. 2A). To obtain an estimate of the AHR protein reduction, a semiquantitative Western blot analysis was performed. To accomplish this, we ran four independent liver samples each from the *Aip^{fx/fx}* and *Aip^{fx/fx}Cre^{alb}* mice. To normalize for loading, we corrected the density measurements for the AHR signal at 104 kDa with the β -actin signal at 44 kDa. From these comparisons, we found that the AHR protein levels were reduced 62% in the liver cytosols of *Aip^{fx/fx}Cre^{alb}* mice (Fig. 2B) ($p < 0.05$).

Differential AHR-mediated Transcription in the Liver of *Aip^{fx/fx}Cre^{alb}* Mice—To assess the impact of hepatocyte *Aip* disruption on the AHR-mediated adaptive response, we measured hepatic mRNA levels of four characteristic AHR-responsive genes (i.e. *Cyp1a1*, *Cyp1a2*, *Cyp1b1*, and *Ahrr*) in *Aip^{fx/fx}* or *Aip^{fx/fx}Cre^{alb}* mice treated with either corn oil or dioxin (Fig. 3, A–D). In dioxin-treated *Aip^{fx/fx}* mice, the *Cyp1a1*, *Cyp1a2*, *Cyp1b1*, and *Ahrr* mRNA levels were induced ~ 10 –1000-fold as compared with corn oil-treated *Aip^{fx/fx}* mice. The induction levels of *Cyp1a1* and *Cyp1a2* mRNA were not significantly different between *Aip^{fx/fx}* and *Aip^{fx/fx}Cre^{alb}* mice treated with dioxin. In contrast, induction levels of both *Cyp1b1* and *Ahrr* mRNA were each decreased by 92% in the liver of dioxin-treated *Aip^{fx/fx}Cre^{alb}* mice relative to dioxin-treated *Aip^{fx/fx}* mice ($p < 0.05$). The different responses of these AHR-responsive genes were also confirmed at the protein levels (Fig. 3E).

***Aip^{fx/fx}Cre^{alb}* Mice Are Resistant to Dioxin-induced Hepatotoxicity—**To investigate the contribution of hepatocyte AIP to dioxin-induced liver toxicity, we compared several dioxin endpoints between *Aip^{fx/fx}* mice and *Aip^{fx/fx}Cre^{alb}* mice. In *Aip^{fx/fx}* mice and *Aip^{fx/fx}Cre^{alb}* mice, liver weights increased $\sim 40\%$ upon treatment with dioxin (Table 2), and thymus weights decreased ~ 50 –60% as compared with controls (Table 2). In contrast, serum ALT activity was significantly increased by dioxin exposure only in the *Aip^{fx/fx}* mice but not in the *Aip^{fx/fx}Cre^{alb}* mice (Table 2). We also assessed the dioxin-induced hepatic damage from the liver sections by staining with hematoxylin and eosin (Fig. 4 and supplemental material). The liver sections of dioxin-treated *Aip^{fx/fx}* mice showed severe hepatocellular hydropic degeneration (zone 2) and areas of focal inflammation consisting of macrophages, lymphocytes, and necrotic cells (Fig. 4 and supplemental material). In contrast to the *Aip^{fx/fx}* mice, none of these dioxin-induced pathological changes were observed in dioxin-treated *Aip^{fx/fx}Cre^{alb}* mice (Fig. 4 and supplemental material).

DISCUSSION

The AIP protein (also known as ARA9 and XAP2) is a known co-chaperone of the AHR signaling pathway (18–21). To assess the importance of AIP in the adaptive, developmental, and toxicological aspects of AHR signaling *in vivo*, we have previously created mice with mutant *Aip* alleles (22, 24). In our earlier studies, we found that *Aip* null (*Aip^{-/-}*) animals died at various prenatal time points due to defects in heart development (22). Although *Aip^{-/-}* mice revealed an essential role for the locus in cardiovascular development, the model was not particularly valuable for use in studying AHR-mediated toxic and adaptive

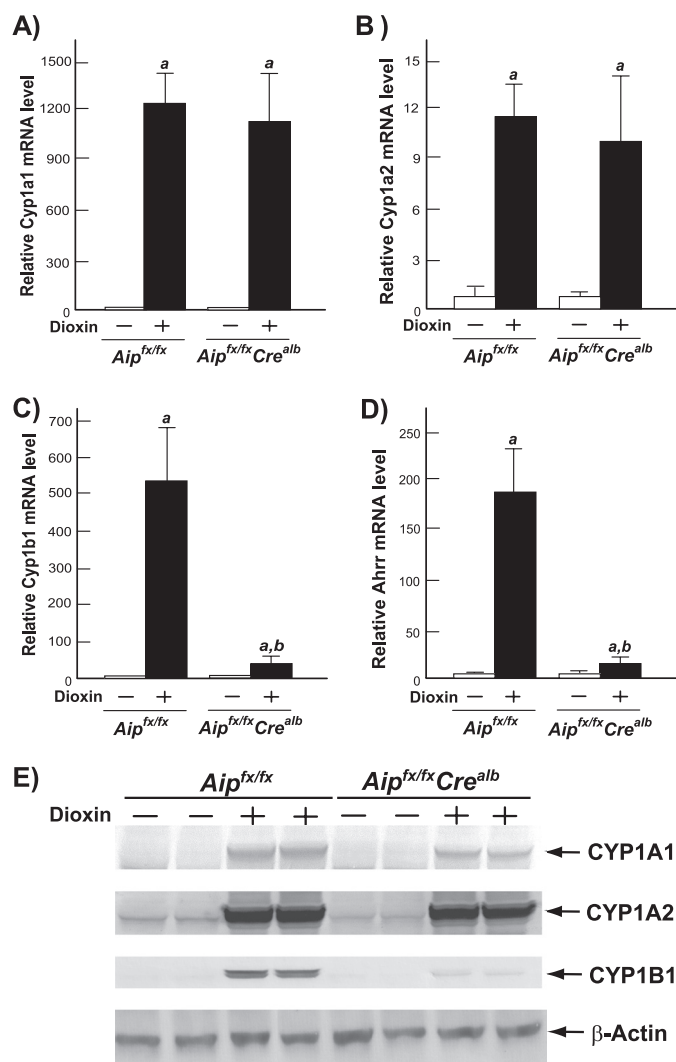


FIGURE 3. Comparison of dioxin-induced adaptive responses between *Aip*^{f/f} and *Aip*^{f/f}*Cre*^{alb} mice. Mice were treated with corn oil or 64 μg/kg of dioxin and sacrificed 5 days after the single i.p. injection. Total RNA was isolated from the liver of the *Aip*^{f/f} and *Aip*^{f/f}*Cre*^{alb} mice. A–D, relative fold induction of AHR gene batteries. A, *Cyp1a1* mRNA; B, *Cyp1a2* mRNA; C, *Cyp1b1* mRNA; D, *Ahrr* mRNA. The mRNA levels of each gene were determined by quantitative RT-PCR, and these measured mRNA levels were normalized to β-actin mRNA level. Results were expressed as relative mRNA level as compared with corn oil-treated *Aip*^{f/f} mice. Each group contained six mice. Open bars, corn oil treatment. Closed bars, dioxin treatment. Error bars represent S.E. a, significantly different relative to the corn oil-treated *Aip*^{f/f} mice ($p < 0.05$). b, significantly different relative to the dioxin-treated *Aip*^{f/f} mice ($p < 0.05$). E, Western blot analysis. Microsomal proteins were isolated from livers of *Aip*^{f/f} and *Aip*^{f/f}*Cre*^{alb} mice. 50 μg of microsomal proteins were analyzed by using CYP1A1, CYP1A2, CYP1B1, and β-actin specific antibodies.

endpoints that are observed in the adult. In a follow-up attempt to overcome the embryonic lethality, we created mice that were hypomorphic for the *Aip* allele (24). These hypomorphic mice survive to adulthood and yet display a global decrease of AIP protein that is ~10–20% of WT mice. Similar to what is seen in mice with *Ahr* or *Arnt* mutant alleles, the *Aip* hypomorphic animals also display a high incidence of patent DV throughout life (8–12, 24). Although these previously generated mice provided evidence to support the idea that the AIP protein plays an important role in the AHR-mediated developmental pathway, the high incidence of patent DV precluded the use of this model in toxicology/pharmacology studies.

To better understand the adaptive and toxicological roles of AIP in AHR biology, we proceeded with the generation of mice with a conditional *Aip* allele that can be excised in a known dioxin target cell, the hepatocyte (25). Through cross-breeding of the conditional *Aip* allele (*Aip*^{f/f}) with mice harboring the albumin promoter-driven *Cre* recombinase, we generated mice that display a tissue-specific deletion of the *Aip* gene in hepatocytes. Unlike previously generated global *Aip* null alleles, these hepatocyte *Aip* null (*Aip*^{f/f}*Cre*^{alb}) mice showed normal heart development and no embryonic lethality (22).

Although the *Aip*^{f/f}*Cre*^{alb} mouse is a significant improvement over the corresponding null and hypomorphic alleles we have generated previously, it has two subtle phenotypes that should be considered in interpretation of related data. First is the observation that these mice have slightly smaller body sizes than their control littermates. Although this weight reduction is only about 10%, it could be a reflection of some metabolic disturbance unrelated to AHR biology. Additionally, although we observed normal dye perfusion in the vast majority of hepatocyte *Aip* null mice, we observed one such mouse with a patent DV. This is quite surprising as we have never seen a patent DV in any of the hundreds of wild-type mice we have phenotyped over the years, and we have never seen a patent DV in the hepatocyte *Ahr* null alleles (25). These observations suggest that AIP in hepatocytes might play a minor role in hepatic vascular development and overall metabolism, perhaps through some parallel PAS (Per-Arnt-Sim) signaling pathways (e.g. hypoxia or circadian).

When we began these experiments, we did not know whether mammalian hepatocytes required AIP for any AHR function or whether redundant chaperones existed within these cells to allow normal receptor folding and stability. To test the idea that the *Aip*^{f/f}*Cre*^{alb} mice would display a loss or reduction of AHR protein, we performed Western blot analysis on whole liver cytosols. We observed that the amount of AHR protein in the liver of *Aip*^{f/f}*Cre*^{alb} mice was reduced more than 60% as compared with control animals (*Aip*^{f/f}) (Fig. 2, A and B), whereas the ARNT protein level was not altered (Fig. 2A). Given that the AHR protein exists in the nonparenchymal cells of the liver and the fact that AHR observed on Western blot may represent improperly folded receptor, it is postulated that the actual reduction of functional AHR in hepatocytes may be even greater than 60%. This assumption will be tested once we establish *in vitro* hepatocyte models derived from these animals.

The observation that the AHR protein is highly expressed only in the presence of AIP is consistent with what we had observed in mammalian cell culture systems, where AIP influenced both the stability and the localization of the receptor (18). We conclude that the decrease of AHR protein in hepatocytes of the *Aip*^{f/f}*Cre*^{alb} mice may result from the loss of the AIP-AHR interaction, leading to a decline in the stability of the AHR protein in the cytosol and a decrease in receptor half-life, possibly due to an increase in its proteasomal degradation (18–21, 32).

Despite the reduced levels of AHR protein in the hepatocytes, the *Aip*^{f/f}*Cre*^{alb} mice displayed normal induction levels of *Cyp1a1* and *Cyp1a2* mRNA in response to the potent agonist dioxin (Fig. 3, A and B). In contrast, induced levels of both

Adaptive and Toxic Role of AIP in Hepatocytes

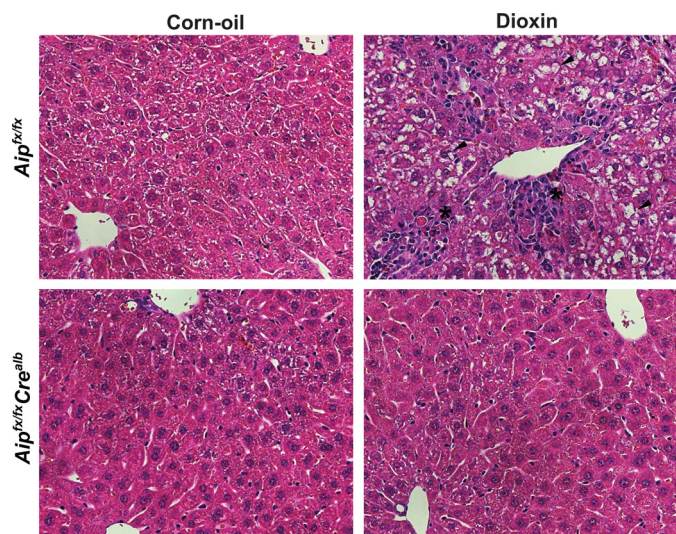


FIGURE 4. *Aip*^{fx/fx} *Cre*^{alb} mice are resistant to dioxin-induced hepatic damage. Mice were treated with corn oil or 64 $\mu\text{g}/\text{kg}$ of dioxin and sacrificed 5 days after the single i.p. injection. The liver sections were stained with hematoxylin and eosin. Magnification, $\times 100$. Black arrowhead, the region of hydropic degeneration; asterisk, focal inflammation.

Cyp1b1 and *Ahrr* mRNA were $\sim 92\%$ lower than those in the dioxin-treated *Aip*^{fx/fx} mice (Fig. 3, C and D). Although we find this differential response of some genes to be potentially of great importance, the dose-response curves for these and other genes will require a more thorough examination to truly understand the underlying mechanisms. Given the high costs associated with mouse models, detailed dose-response studies may be best performed in hepatocyte cell culture systems, where the dose-response curves of responsive genes can be compared under varying concentrations of AHR, ARNT, and AIP.

The simplest interpretation of the differential induction data is that different DRE-driven genes are differentially responsive to varying levels of available AHR in the cell. For example, the reduced responsiveness of *Cyp1b1* observed in *Aip* mutants may be related to the reduced number of receptors available for activation by ligand. In line with this idea, the lower AHR concentrations in the *Aip* mutants may still be large enough to fully occupy "high affinity/availability" DREs within the genome, but the smaller pool of available receptors in *Aip* mutants is not large enough to fully occupy lower affinity enhancers. Data supporting the idea that different target genes may harbor differential responsiveness to the AHR include previous reports that the ED₅₀ for dioxin exposure using *Cyp1b1* induction in liver as an end point is 3–24-fold higher than that for *Cyp1a1* or *Cyp1a2* induction (33–35).

An alternative model is that AIP may be required to couple the AHR to certain DREs and not others. For example, one can predict a scenario where AIP-dependent AHR folding influences receptor phosphorylation. In turn, this phosphorylation event could then influence gene expression from some target promoters (*i.e.* *Cyp1b1*) and not others (*i.e.* *Cyp1a1*), resulting in differential responsiveness. Alternatively, AIP may couple the AHR to specific coactivators required to drive the transcription of select DRE-coupled target genes.

The observation of differential dependence of gene expression on the number of activated receptors in the cell has potential to help us understand the mechanism of dioxin-induced hepatotoxicity. If this observation can be better understood, it may guide us to the identification of those gene batteries that have a greater probability of being at the root cause of dioxin-induced hepatocellular damage. That is, hepatocellular damage as reported by ALT release, steatosis, and lymphoid infiltration may be directly mediated by AIP-dependent AHR signaling. In contrast, other toxic endpoints such as liver enlargement may be mediated in an AIP-independent manner. This idea suggests that a search for AIP-dependent gene targets may reveal the ultimate transcriptional targets of the dioxin-AHR complex as they relate to hepatocellular damage and perhaps even cancer. Moreover, it might be an indication that AIP-interactions may be an important determinant of individual, cross-species, and organotropic toxicity. Perhaps this determinant could be as important or even more important than differential ligand binding affinity.

CONCLUSION

We have generated a hepatocyte-specific *Aip* null mouse model that provides a number of important insights into AHR biology. Of greatest interest to us is the observation that loss of the AIP protein in the hepatocyte leads to reduction in levels of AHR protein and eliminates/reduces dioxin hepatotoxicity as defined by hepatocellular damage and ALT release. The observation that up-regulation of *Cyp1a1* and *Cyp1a2* still occurs normally in this model supports the uncoupling of the *Cyp1a1/Cyp1a2* response from many aspects of dioxin toxicity. This model also provides a potential approach to define those genes directly mediating dioxin toxicity. That is, genes that mediate toxic endpoints such as hepatocellular damage may be dependent upon AIP co-expression.

Acknowledgments—We thank Xiaojing Zhang for performing the quantitative RT-PCR and Anna L. Shen and Brian P. Johnson for reviewing the manuscript.

REFERENCES

- Hankinson, O. (1995) *Annu. Rev. Pharmacol. Toxicol.* **35**, 307–340
- Gu, Y. Z., Hogenesch, J. B., and Bradfield, C. A. (2000) *Annu. Rev. Pharmacol. Toxicol.* **40**, 519–561
- Pohjanvirta, R., and Tuomisto, J. (1994) *Pharmacol. Rev.* **46**, 483–549
- Whitlock, J. P., Jr., Chichester, C. H., Bedgood, R. M., Okino, S. T., Ko, H. P., Ma, Q., Dong, L., Li, H., and Clarke-Katzenberg, R. (1997) *Drug Metab. Rev.* **29**, 1107–1127
- Whitlock, J. P., Jr. (1999) *Annu. Rev. Pharmacol. Toxicol.* **39**, 103–125
- Nebert, D. W., and Gonzalez, F. J. (1987) *Annu. Rev. Biochem.* **56**, 945–993
- Baba, T., Mimura, J., Gradin, K., Kuroiwa, A., Watanabe, T., Matsuda, Y., Inazawa, J., Sogawa, K., and Fujii-Kuriyama, Y. (2001) *J. Biol. Chem.* **276**, 33101–33110
- Lahvis, G. P., Lindell, S. L., Thomas, R. S., McCuskey, R. S., Murphy, C., Glover, E., Bentz, M., Southard, J., and Bradfield, C. A. (2000) *Proc. Natl. Acad. Sci. U.S.A.* **97**, 10442–10447
- Bunger, M. K., Moran, S. M., Glover, E., Thomae, T. L., Lahvis, G. P., Lin, B. C., and Bradfield, C. A. (2003) *J. Biol. Chem.* **278**, 17767–17774
- Walisser, J. A., Bunger, M. K., Glover, E., and Bradfield, C. A. (2004) *Proc. Natl. Acad. Sci. U.S.A.* **101**, 16677–16682
- Harstad, E. B., Guite, C. A., Thomae, T. L., and Bradfield, C. A. (2006) *Mol.*

- Pharmacol.* **69**, 1534–1541
12. Walisser, J. A., Bunger, M. K., Glover, E., Harstad, E. B., and Bradfield, C. A. (2004) *J. Biol. Chem.* **279**, 16326–16331
 13. Carver, L. A., and Bradfield, C. A. (1997) *J. Biol. Chem.* **272**, 11452–11456
 14. Whitelaw, M. L., Göttlicher, M., Gustafsson, J. A., and Poellinger, L. (1993) *EMBO J.* **12**, 4169–4179
 15. Petrusis, J. R., and Perdew, G. H. (2002) *Chem. Biol. Interact.* **141**, 25–40
 16. Ma, Q., and Whitlock, J. P., Jr. (1997) *J. Biol. Chem.* **272**, 8878–8884
 17. Kuzhandaivelu, N., Cong, Y. S., Inouye, C., Yang, W. M., and Seto, E. (1996) *Nucleic Acids Res.* **24**, 4741–4750
 18. LaPres, J. J., Glover, E., Dunham, E. E., Bunger, M. K., and Bradfield, C. A. (2000) *J. Biol. Chem.* **275**, 6153–6159
 19. Meyer, B. K., Pray-Grant, M. G., Vanden Heuvel, J. P., and Perdew, G. H. (1998) *Mol. Cell. Biol.* **18**, 978–988
 20. Meyer, B. K., and Perdew, G. H. (1999) *Biochemistry* **38**, 8907–8917
 21. Petrusis, J. R., Hord, N. G., and Perdew, G. H. (2000) *J. Biol. Chem.* **275**, 37448–37453
 22. Lin, B. C., Sullivan, R., Lee, Y., Moran, S., Glover, E., and Bradfield, C. A. (2007) *J. Biol. Chem.* **282**, 35924–35932
 23. Schmidt, J. V., Su, G. H., Reddy, J. K., Simon, M. C., and Bradfield, C. A. (1996) *Proc. Natl. Acad. Sci. U.S.A.* **93**, 6731–6736
 24. Lin, B. C., Nguyen, L. P., Walisser, J. A., and Bradfield, C. A. (2008) *Mol. Pharmacol.* **74**, 1367–1371
 25. Walisser, J. A., Glover, E., Pande, K., Liss, A. L., and Bradfield, C. A. (2005) *Proc. Natl. Acad. Sci. U.S.A.* **102**, 17858–17863
 26. Dymecki, S. M. (1996) *Proc. Natl. Acad. Sci. U.S.A.* **93**, 6191–6196
 27. Farley, F. W., Soriano, P., Steffen, L. S., and Dymecki, S. M. (2000) *Genesis* **28**, 106–110
 28. Postic, C., Shiota, M., Niswender, K. D., Jetton, T. L., Chen, Y., Moates, J. M., Shelton, K. D., Lindner, J., Cherrington, A. D., and Magnuson, M. A. (1999) *J. Biol. Chem.* **274**, 305–315
 29. Thomas, R. S., Penn, S. G., Holden, K., Bradfield, C. A., and Rank, D. R. (2002) *Pharmacogenetics* **12**, 151–163
 30. Nukaya, M., Moran, S., and Bradfield, C. A. (2009) *Proc. Natl. Acad. Sci. U.S.A.* **106**, 4923–4928
 31. Savas, U., Bhattacharyya, K. K., Christou, M., Alexander, D. L., and Jefcoate, C. R. (1994) *J. Biol. Chem.* **269**, 14905–14911
 32. Kazlauskas, A., Poellinger, L., and Pongratz, I. (2000) *J. Biol. Chem.* **275**, 41317–41324
 33. Abel, J., Li, W., Döhr, O., Vogel, C., and Donat, S. (1996) *Arch. Toxicol.* **70**, 510–513
 34. Santostefano, M. J., Ross, D. G., Savas, U., Jefcoate, C. R., and Birnbaum, L. S. (1997) *Biochem. Biophys. Res. Commun.* **233**, 20–24
 35. Walker, N. J., Portier, C. J., Lax, S. F., Crofts, F. G., Li, Y., Lucier, G. W., and Sutter, T. R. (1999) *Toxicol. Appl. Pharmacol.* **154**, 279–286